Unsaturated Soils for Asia, Rahardjo, Toll & Leong (eds) © 2000 Balkema, Rotterdam, ISBN 90 5809 139 2

# The application of knowledge-based surface flux boundary modelling

G.W.Wilson & M.D.Fredlund
*Department of Civil Engineering, University of Saskatchewan, Saskatoon, Sask., Canada*

ABSTRACT: The moisture flux boundary condition at the ground surface is dynamic and continuously driven by atmospheric forcing events. The application of the SoilCover model to predict the flux boundary conditions for two soil cover systems is demonstrated in this paper. A knowledge-based system is used to predict the soil-water characteristic curves and associated soil property functions required for the SoilCover model. A case study for the Saskatoon landfill is reviewed. The analyses show that both soil properties and climate parameters are paramount. The final approach used for the design of any ground surface profile to control flux boundary conditions must include climatic parameters together with hydraulic properties of the soil profile.

## 1 INTRODUCTION

Geotechnical engineers are frequently called upon to design soil cover systems for the management of solid waste systems. The closure of municipal landfills is an important application for cover system design. In general terms, the primary function of the cover system is to control the net infiltration rate to the underlying waste that produces leachate at the base of the landfill. This paper illustrates the application of two computer models for the design of a soil cover system for a landfill situated in the City of Saskatoon, Canada. Surface flux boundary conditions for two potential cover profiles are evaluated using the SoilCover (1997) model. A newly developed knowledge based program system (Fredlund et al, 1998) is used to estimate the soil property functions necessary to run the SoilCover model.

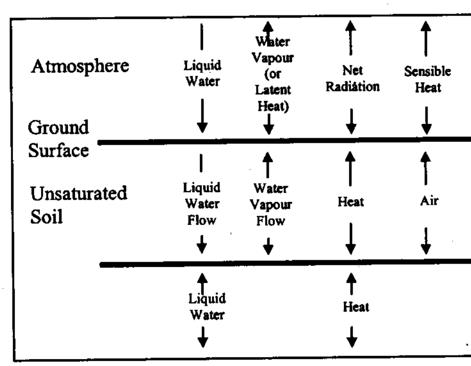


Figure 1. One dimensional view of fluxes in the soil-atmosphere profile.

## 2 THEORY

The moisture flux boundary condition is dynamic and continuously driven by atmospheric forcing conditions. Infiltration and evaporation across the soil/atmosphere boundary are a function of precipitation and potential evaporation as well as soil properties. Fluxes within the soil/atmosphere continuum are fully coupled in terms of heat and mass transfer. The flow of liquid water, water vapour, air and heat is shown in Figure 1.

The general equation for the flow of liquid water and water vapour are given by Wilson et al. (1997) as follows:

$$\frac{\partial h_w}{\partial t} = C_w^1 \frac{\partial}{\partial y}\left[k_w \frac{\partial h_w}{\partial y}\right] + C_w^2 \frac{\partial}{\partial y}\left[D_v \frac{\partial P_v}{dy}\right] \qquad (1)$$

where $h_w$ = hydraulic head (m); $C_w^1$ = modulus of volume change with respect to the liquid water phase $(1/\rho_w g m_w^2)$; $C_w^2$ = modulus of volume change with respect to water vapour phase $[(P + P_v)/P(\rho_w)^2 g m_w^2]$; $D_v$ = coefficient of diffusion for water vapour through soil (kg-m/kN-s); $\rho_w$ = density of liquid water (kg/m$^3$); $g$ = acceleration due to gravity (m/s$^2$); $m_w^2$ = slope of the soil-water characteristic curve (1/kPa); $P$ = total atmosphereic pressure (kPa); and $P_v$ = partial pressure in the soil due to water vapour (kPa).

Conductive heat flow is coupled with the interphase flux of liquid water and water vapour as follows:

$$C_h \frac{\partial T}{\partial y} = \frac{\partial}{\partial y}\left(\lambda \frac{\partial T}{\partial y}\right) - L_v\left(\frac{P+P_v}{P}\right)\frac{\partial}{\partial y}\left(D_v \frac{\partial P_v}{\partial y}\right) \quad (2)$$

where $C_h$= volumetric spcific heat (J/m$^3$-°C); $T$ = temperature (°C); $\lambda$ = thermal conductivity (W/m-°C); and $L_v$ = latent heat of vapouriztion (J/kg).

Infiltration events are simulated by applying a liquid flux equal to the rainfall intensity to the right side of equation 1. This procedure is straight forward. Alternatively the solution for evaporation events is more complex since the rate of actual evaporation is a function of both the rate of potential evaporation and the suction in the soil at the ground surface. The actual rate of evaporation is equal to the potential rate of evaporation until the value of suction at the soil surface exceeds approximately 3000 kPa. The value of actual evaporation progressively decreases during desiccation with increasing suction once the soil suction exceeds 3000 kPa. The decline in evaporation occurs due to depression of the vapour pressure within the voids of the soil with increasing suction. The relationship for relative humidity and suction given by Edlefsen and Anderson (1943) is shown in Figure 2 and written as:

$$RH = e^{\frac{\psi W_v}{RT}} \quad (3)$$

where $RH$ = relative humidtiy of the soil surface as a function of total suction; $\psi$ = total suction in the soil (kPa); $W_v$ = Molecular weight of water (0.018 kg/mole); $R$ = universal gas constant (8.314 J/mole/°K); and $T$ = absolute temperature (°K).

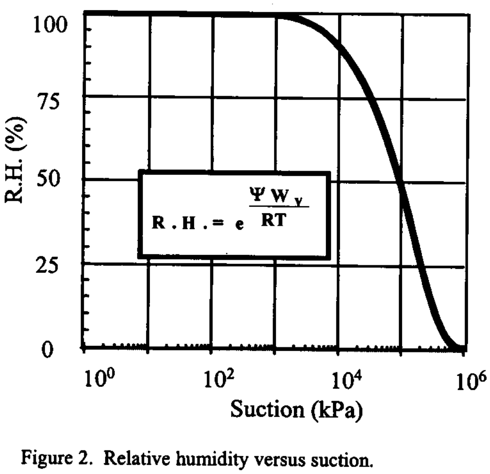


Figure 2. Relative humidity versus suction.

The relationship between actual evaporation (AE) and suction is universal for all soil types. Wilson et al. (1997) showed that the relationship is independent of soil texture for sand, silt and clay as shown in Figure 3. This is an important point to note since the term for suction can be defined as a stress state variable that controls the evaporative flux from a given soil surface.

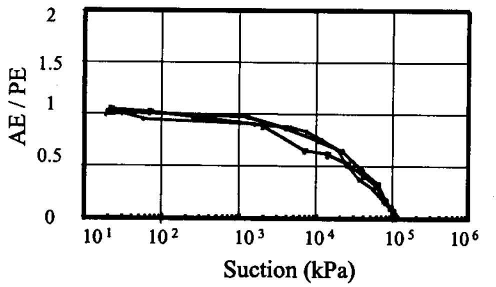


Figure 3. Ratio of actual evaporation and potential evaporation as a function of soil suction for a sand, silt and clay (after Wilson et al., 1997).

The principle outlined above may be used to modify the Penman (1948) method for potential evaporation (PE) to compute actual soil evaporation (AE) as follows (Wilson et al. 1994):

$$E = \frac{\Delta Q_n + \gamma E_a}{\Delta + A} \quad (4)$$

where $E$ = evaporative flux (mm/day); $\Delta$ = slope of the saturation vapour pressure versus temperature curve at the mean temperature of the air (mmHg/°C); $Q_n$ = net radian energy available at the surface (mm/day); $\gamma$ = psychrometric constant; and

$E_a = f(u)e_a(B-A)$ (4a)

where $f(u)$ = 0.35 (1 + 0.146 $Wa$); $Wa$ = wind speed (km/h); $e_a$= water vapour pressure of the air above the soil surface (mmHg); $B$ = inverse of the relative humidity in the air; and $A$ = inverse of the relative humidity at the soil surface.

The solution for the system of equations 1 through 4 requires that the temperature for the soil surface be defined. Surface temperature is computed as follows:

$$T_s = T_a + \frac{1}{\gamma(f(u))}(Q_n - E) \quad (5)$$

where $T_s$ = temperature of the soil surface (°C); and $T_a$ = air temperature above the soil surface (°C).

The solution for equations 1 through 5 outlined above is provided by the SoilCover (1997) computer model. Root-water uptake due to plant transpiration must also be included if the soil surface is vegetated. The method described by Tratch et al. (1995) and Ritchie (1972) is utilized in the SoilCover (1997) model.

## 3 APPLICATION OF THE KNOWLEDGE-BASE SYSTEM

The SoilCover (1997) model requires detailed input for the specification of soil properties and climatic parameters. Information for the climatic parameters can be obtained from routine weather station installations. The parameters include daily precipitation, net radiation, maximum and minimum temperature and relative humidity, wind speed and pan evaporation. In many cases this data can be easily obtained from government agencies (i.e., regional meteorological station and airports, etc.). The evaluation of soil properties is more difficult.

Soil property functions for the soil-water characteristic curve and the saturated/unsaturated hydraulic conductivity function are required as input parameters for the SoilCover model. The soil property functions may be measured in the laboratory using pressure plates and permeameters. These laboratory test procedures are expensive and often require several weeks to complete. In many cases, several soils must be evaluated. A knowledge-based system may be used to assist in the evaluation for a range of materials that are available for the design and construction of the cover. Application of the knowledge-based system described by Fredlund et al. (1998) for the selection of cover materials is demonstrated here.

Figure 4 shows the grain-size distribution for four potential material types that are available for construction of a cover system. The predicted soil-water characteristic curves given by the knowledge-base system (Fredlund et al. 1998) for each material can be seen in Figure 5. The clay material has an air entry value (AEV) greater than 100 kPa together with a low value of saturated hydraulic conductivity in the range of 1 x $10^{-10}$ cm/sec. In many cases this type of material is suitable for the construction of a sealing layer. However, a compacted clay cover system is not considered suitable for the semi-arid climate of Saskatoon. Experience has shown that this type of material is subject to shrinkage and cracking during dry periods. This will result in a loss of integrity with respect to restricting water infiltration. It can also be seen in Figure 5 that the AEV for the gravel is less than 1 kPa and that the suction at which the residual water content is reached is approximately 3 kPa. The high permeability and poor water retention characteristics eliminate this material as a potential cover material.

The soil-water characteristic curves for the fine sand and silty loam suggest these soils may be suitable for the construction of a cover system. Figure 5 shows the AEV and the suction at residual water content for the fine sand to be 7 and 100 kPa respectively. The AEV for the silty loam is lightly higher. The gentle slope of the SWCC with increasing soil suction indicates this material will have excellent water retention characteristics for a store and release cover system. The fine sand and silty loam were therefore selected for laboratory testing based on the results of the predictions of the knowledge-based system. In summary, the number of pressure plate tests was reduced to two soil types from the original four samples.

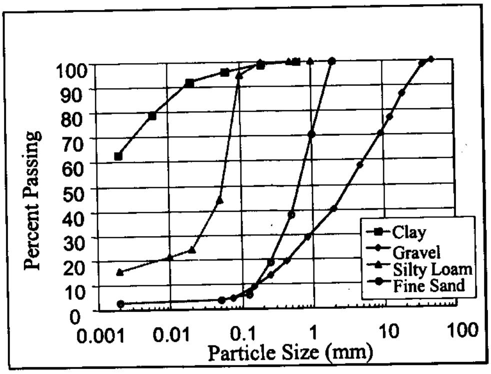


Figure 4. Grain-size distribution for four soil types available for cover construction.

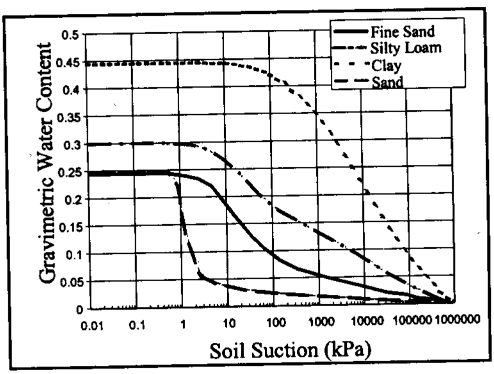


Figure 5. Predicted soil-water characteristic curves determined by the knowledge-based system.

## 4 SOILCOVER MODEL RESULTS

Figures 6 and 7 show the measured SWCC and estimated hydraulic conductivity function for the fine

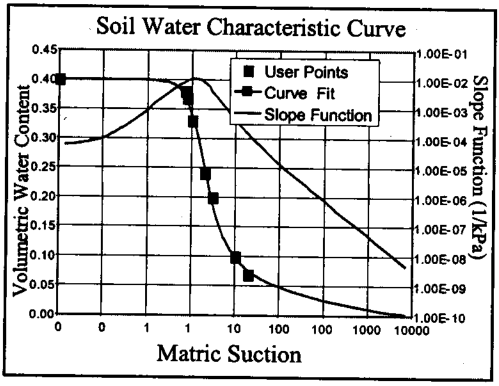


Figure 6. Soil-water characteristic curve for the fine sand specified in the SoilCover model.

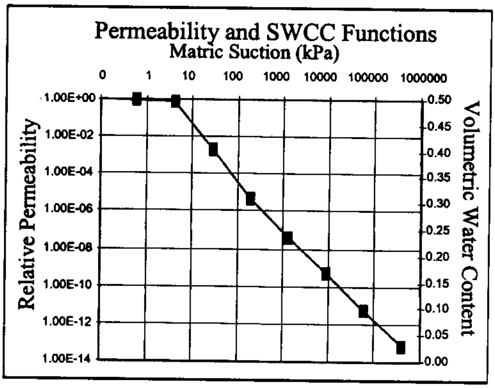


Figure 7. Hydraulic conductivity function for the cover material based on the Fredlund and Xing method.

sand. The hydraulic conductivity function was determined on the basis of the Fredlund and Xing (1994) method. The saturated hydraulic conductivity of the sand was measured to be 3 x $10^{-5}$ m/sec.

Figures 8 and 9 show the SWCC and hydraulic conductivity function for the fine sandy loam. The saturated hydraulic conductivity of the fine sandy loam was measured to be 1 x $10^{-7}$ m/sec. The soil property functions illustrated in Figures 6 through 9 were used to predict infiltration rates for two 1.5 m thick cover systems.

Figure 10 illustrates the cumulative ground surface fluxes for a 1.5 m sand cover at the Saskatoon landfill after approximately 150 days. The data for precipitation was obtained from historic meteorological data for the year 1993. It can be seen in Figure 10 that the total precipitation for the simulation period is 400 mm while potential evaporation is approximately double this value at 750 mm. Figure 10 shows the cumulative actual evaporation of 350 mm to be significantly less than the potential evaporation. This leaves the amount of water available

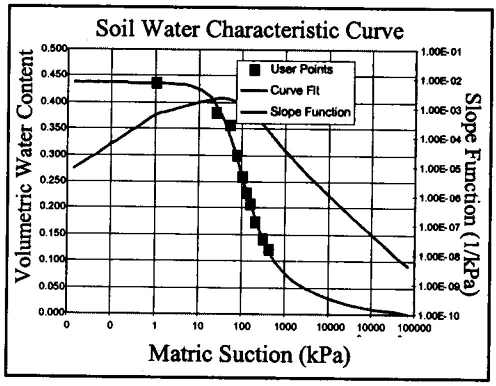


Figure 8. Soil-water characteristic curve for the fine sandy loam material specified in the SoilCover model.

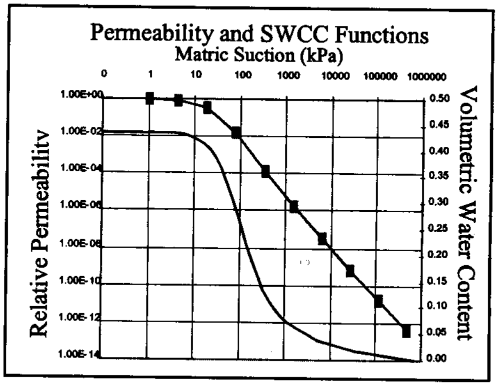


Figure 9. Hydraulic conductivity function for the fine silty loam material based on the Fredlund and Xing method.

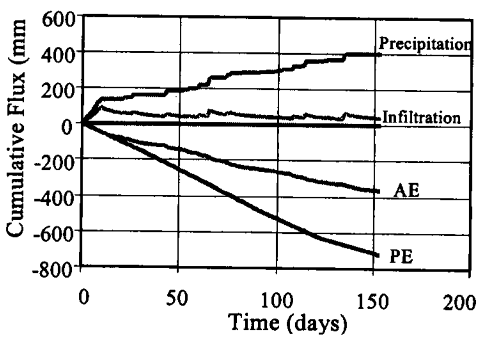


Figure 10. Cumulative fluxes for sand cover.

for infiltration equal to approximately 50 mm or about 10% of total precipitation.

Figure 11 shows the water content profiles for the 1.5 m thick sand cover on days 0, 10, 65 and 150. It can be seen that a wetting front advances through the profile on day 10 of the simulation followed by a second wetting period on day 65. This shows that significant quantities of water readily infiltrate through the sand cover. In summary, the performance of the sand cover system is considered unacceptable.

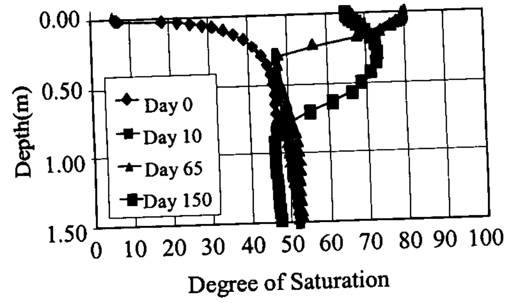


Figure 11. Water content profile for sand cover.

Figure 12 shows the cumulative ground surface fluxes for a cover system consisting of 1.0 m of silty loam over 0.5 m of fine sand. The climate data used for the simulation was exactly the same as that used for the previous analysis. It can be seen in Figure 12 that the net infiltration is reduced to zero for the 150 day period. This occurs as a result of the higher value of actual evaporation (AE) equal to approximately 400 mm. The performance of this cover system shows significant improvement compared to the homogeneous 1.5 m sand profile.

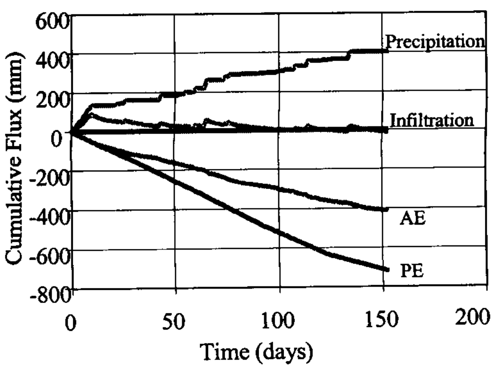


Figure 12. Cumulative fluxes for silt over sand cover.

Figure 13 presents the computed volumetric water content profiles for the 1.0 m silt over 0.5 m sand cover profile. It can be seen that the silty loam material maintains a relatively high value of water saturation. This can be attributed to the higher air entry value and water retention capacity of this material compared to the sand. The net result in retaining more soil water near the ground surface provides a higher value of actual evaporation. This translates to a reduction in net infiltration equal to a value approaching zero. The silty loam profile in the cover performs as a store and release cover system. Infiltration water that enters the soil profile early in the simulation period (actually a result of snow melt during the spring) is retained near the ground surface for a sufficient period of time such that it may be removed during the high evaporation period that occurs during the summer months. In summary, the analyses show that a material with a moderately low value of hydraulic conductivity (i.e., 1 x $10^{-7}$ m/sec) such as silt can provide a barrier to infiltration in semi-arid climates with wet and dry periods.

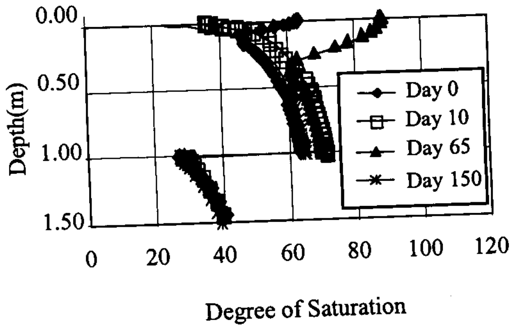


Figure 13. Water content profile for the silt over sand cover.

## 5 CONCLUSIONS

The application of the SoilCover model to the design of a soil cover system for a municipal landfill was demonstrated. The results of the simulation show that a silty loam material provides a barrier to infiltration in the semi-arid climate that prevails in Saskatoon. It is interesting to note that a silt rich material can provide better protection against infiltration than a highly plastic clay material since severe cracking associated with desiccation is avoided. The numerical modelling and design of the cover system was assisted with the use of a knowledge base system for the selection of suitable soils of testing and analysis. This approach reduced the amount of laboratory testing and time required to complete the analysis.

## REFERENCES

Edlefsen, N.E. & Anderson, A.B.C. 1943. *Thermodynamics of Soil Moisture*, Hilgardia, 15(2), pp. 31-298.

Fredlund, D.G. & Xing Anqing, 1994. Predicting the permeability for Unsaturated Soils Using the Soil-Water Characteristic Curve. *Canadian Geotechnical Journal*, Vol.31, pp. 521-532.

Fredlund, M.D., Wilson, G.W., & Fredlund, D.G., 1998. Estimation of Hydraulic Properties of An Unsaturated Soil Using A Knowledge-Based System, *Second International Conference on Unsaturated Soils*, August 27-30.

Penman, H.L., 1948. Natural Evaporation From Open Water, Bare Soil and Grass. *Proceedings of the Royal Society of London, Series A,* 193; pp. 120-146.

Ritchie, J.T., 1972. Model for Predicting Evaporation From a Row Crop with Incomplete Cover. *Water Resources Research*, 8(5): 1204-1213.

SoilCover, 1997. *User's Manual,* Unsaturated Soils research Group, Department of Civil Engineering, University of Saskatchewan, Saskatoon, Canada.

Tratch, D.J., Wilson, G. W. & Fredlund, D.G., 1995. An Introduction to Analytical Modelling of Plant Transpiration For Geotechnical Engineers. *Proceedings of the 48th Annual Canadian Geotechnical Conference, Vancouver, BC,* September 25-27, pp. 771-780.

Wilson, G.W., Fredlund, D.G. & Barbour, S.L., 1997. The effect of soil suction of evaporative fluxes from soil surfaces. *Canadian Geotechnical Journal* (34), pp.145-155.